

Non-dimensional Star-Identification

Carl Leake*, David Arnas† and Daniele Mortari‡

Abstract

This study introduces a new “Non-Dimensional” star identification algorithm to reliably identify the stars observed by a wide field-of-view star tracker when the focal length and optical axis offset values are known with poor accuracy. This algorithm is particularly suited to complement nominal lost-in-space algorithms when they fail the star identification due to focal length and/or optical axis offset deviations from their nominal operational ranges. These deviations may be caused, for example, by launch vibrations or thermal variations in orbit. The algorithm performance is compared in terms of accuracy, speed, and robustness to the Pyramid algorithm. These comparisons highlight the clear advantages that a combined approach of these methodologies provides.

1 Introduction

If a star tracker is working as intended, a nominal lost-in-space (NLISA) star identification (Star-ID) algorithm can be used to identify stars using only the observed directions of the unknown stars and a star catalog. These algorithms are paramount for determining the attitude of a spacecraft using a star tracker. In terms of speed and robustness, the state-of-the-art algorithm to identify stars in the nominal lost-in-space scenario is the NLISA Pyramid [1]. The Pyramid algorithm recognizes observed stars using the invariance of the angles between observed and cataloged stars. The k -vector range searching technique [2, 3] is the internal engine of Pyramid that facilitates a quick and robust Star-ID. The Pyramid algorithm is summarized as follows:

1. First, the algorithm searches for a unique star triangle. A unique star triangle consists of three stars whose interstellar angles, the angle between a pair of stars, could only form that particular star triangle. In other words, after merging the results of three searches, one for each of the three star pairs, in a database of interstellar angles, only one possible star triangle emerges. The searches in the interstellar angle database are range searches where the range is based on three standard deviations of the star tracker’s centroiding uncertainty. Let the three stars that make up the unique star triangle be denoted as the i , j , and k stars. If no unique star triangle is found, then the algorithm reports that it cannot identify any stars.
2. Next, Pyramid searches for a reference star, r . A reference star r is any star in the field-of-view such that the $\{i, j, r\}$, $\{i, k, r\}$, and $\{j, k, r\}$ star triangles are unique star triangles. If a reference star is found, then the i , j , k , and r stars are considered identified. They represent the four vertices of a “Pyramid.” If no reference star is found, then the algorithm returns to step one to try to identify a different unique star triangle.
3. Finally, Pyramid identifies or discards the remaining stars using the $\{i, j, k\}$ star triangle and the same technique as the reference star. For a given star s , if the $\{i, j, s\}$, $\{i, k, s\}$, and $\{j, k, s\}$ star triangles are unique star triangles, then the star s is identified. Otherwise, it is discarded.

One issue with NLISA algorithms like Pyramid is that they require an accurate estimate of the star tracker’s focal length and optical axis (OA) offset. However, during a spacecraft’s lifetime, environmental effects such as temperature and vibrations may perturb the focal length and OA offset of the star tracker. When this happens, the Pyramid algorithm may become unable to identify stars or, potentially worse, identify

* Aerospace Engineering, Texas A&M University, College Station, TX 77843-3141, USAleakec@tamu.edu

† Postdoctoral Associate, Department of Aeronautics and Astronautics, Massachusetts Institute of Technology, Cambridge, MA. arnas@mit.edu

‡ Aerospace Engineering, Texas A&M University, College Station, TX 77843-3141, USAmortari@tamu.edu

stars incorrectly. Hence the need for a Star-ID algorithm that is less sensitive to these changes in camera parameters.

To that end, previous algorithms [4, 5, 6, 7] have proposed solutions based on the non-dimensional Star-ID problem, that is, the identification of stars when the focal length or OA offset of the star-tracker have been perturbed from their nominal values. However, these algorithms present an important limitation; they require star catalogues with few stars. In particular, they are designed for star trackers with a small star catalog obtained by either selecting only a few stars from the main catalog, as is done in Ref. [7], or by using a star tracker with a narrow field-of-view, as is done in Refs. [4, 5, 6]. For instance, Ref. [4] deals with narrow field-of-view star trackers and uses the maximum angle of planar star triangles to perform the non-dimensional Star-ID. However, if the field-of-view of the star tracker becomes too wide, the resultant non-dimensional star catalog becomes so populated that the difference in angles between adjacent entries are smaller than the centroiding accuracy of the camera. As a result, it becomes nearly impossible to identify a unique star triangle, and thus, the algorithm cannot identify any stars.

This article proposes the *non-dimensional Star-ID algorithm* (NDSIA), a non-dimensional algorithm that is able to handle much larger star catalogs efficiently. This is accomplished by using the dihedral angles (spherical angles) of star triangles rather than the angles of planar triangles, and by considering a database composed of all three spherical triangle angles rather than just one of the planar triangles' angles. These two changes prevent the non-dimensional catalog from becoming too populated; the problem that plagued previous works. As a consequence of these modifications, NDSIA must perform orthogonal range searches in a three-dimensional database, as opposed to previous algorithms that only dealt with one-dimensional databases. In general, searching in multidimensional databases is significantly more time-consuming due to the increase in the amount of data, and the lack of a clear ordering methodology for multidimensional elements (i.e. in one dimension it is clear how to sort numerical elements so they can be extracted easily, for example in ascending order, but in n -dimensions such a sorting process is more convoluted). Fortunately, recent advances in the n -dimensional k -vector [8] make the searching process viable for real-time applications. As an example of that, this work shows that NDSIA takes milliseconds or tens of milliseconds to run, depending on the perturbations of the star tracker parameters.

The remainder of the article is organized as follows. First, the theory for the NDSIA is introduced. Then, a comparison is made between NDSIA and Pyramid for eight different scenarios, each with different camera perturbations. These eight scenarios showcase the performance of NDSIA when subject to focal length and OA offset perturbations.

2 The Non-dimensional Star-ID Algorithm

Due to thermal and vibrational perturbations, the nominal values of the camera focal length, f , and OA offset, $[x_{oa}, y_{oa}]$, may differ from their nominal values. If this is the case, NLISA (nominal lost-in-space algorithms, e.g., Pyramid [1]) may fail. When this happens, the Star-ID process must be accomplished by an algorithm that is robust to small focal length and OA offset variations. Such an algorithm is presented here; the algorithm is called the non-dimensional Star-ID algorithm (NDSIA). It is important to note at this point that NDSIA is meant to be a backup Star-ID algorithm that is used only when the Pyramid algorithm begins to fail. NDSIA is not meant to replace Pyramid when the star tracker is working nominally, as it requires more memory and a larger computational effort than Pyramid, and it does not provide any benefits when compared with Pyramid under nominal star tracker conditions. As an added benefit, once enough stars are identified using NDSIA, the actual focal length and OA offset of the camera can be calculated, as shown in Ref. [4]. Once these quantities are obtained, a new star database can be generated so that Pyramid can be used again.

The non-dimensional algorithm presented here is reminiscent of the non-dimensional algorithms presented in Refs. [4, 5, 6, 7, 9]. Nevertheless, the non-dimensional algorithm introduced in this work has three major differences when compared with these previous algorithms:

1. NDSIA uses the dihedral angles of spherical star triangles rather than using the planar angles of star triangles as in Refs. [4, 5, 6, 7] or the sides of planar star triangles as in Ref. [9].
2. NDSIA uses the n -dimensional k -vector (NDKV) [8] to search amongst a three-dimensional database, rather than using the one-dimensional k -vector [3] to search amongst a one-dimensional database, as is done in Refs. [4, 5, 6, 7, 9].

- NDSIA performs a final check that uses the identified stars' interstellar angles to further the confidence in the Star-ID. This check is non-existent in Refs. [4, 5, 6, 7, 9].

In previous works, planar star triangles were used to identify stars, because planar triangles are more insensitive to camera perturbations than the interstellar angles used in Pyramid. The dihedral angles of spherical triangles also have this property. However, the dihedral angles of spherical triangles contain more information than planar triangle angles. The missing information on planar triangles is caused by the fact that planar triangles are the projections on a plane of spherical triangles. A more mathematically rigorous way of stating this is planar triangle angles are subject to the constraint that the sum of the angles must be equal to 180° . Thus, each planar triangle only contains two independent pieces of information. In contrast, spherical triangles do not have this constraint. In fact, the sum of spherical triangle angles is in the range $(180^\circ, 540^\circ)$. A numerical study was performed to identify which positions in an image with a given size and focal length generate the largest sum of the three dihedral angles when projected onto the unit sphere. The numerical study concluded that the maximum sum of the three dihedral angles occurs when the three stars are on the border of the image, but their exact positions depend on the image size and the focal length. In summation, each of the three spherical triangle angles provides an independent piece of information. Hence, more information is available when observing three stars as a spherical triangle rather than as a planar triangle.

Previous works were only able to search a one-dimensional database quickly enough for real-time applications. Thus, they were not even able to use all of the information available in planar triangles, let alone the information in spherical triangles. Hence, previous works used planar triangles rather than spherical triangles. However, recent advances in the NDKV have lifted the one-dimensional database restriction. Consequently, the information from all three dihedral angles of spherical triangles can be used to uniquely identify stars. Leveraging this information allows for more entries in the non-dimensional database than in previous works.

2.1 Creating the Non-Dimensional Database

This section presents the database structure used by NDSIA and shows how it is generated. NDSIA uses a database, called the non-dimensional database, composed of dihedral angles of spherical star triangles and their corresponding stars. A visual representation of the dihedral angles of spherical star triangles and a detailed description of how they are calculated is shown in Appendix A. The database is organized according to Table 1.

Table 1: Non-dimensional database layout

	Star Triangle 1	Star Triangle 2	...	Star Triangle n
Row 1	Smallest Dihedral Angle	Smallest Dihedral Angle	...	Smallest Dihedral Angle
Row 2	Middle Dihedral Angle	Middle Dihedral Angle	...	Middle Dihedral Angle
Row 3	Largest Dihedral Angle	Largest Dihedral Angle	...	Largest Dihedral Angle
Row 4	Star Associated with Smallest Dihedral Angle	Star Associated with Smallest Dihedral Angle	...	Star Associated with Smallest Dihedral Angle
Row 5	Star Associated with Middle Dihedral Angle	Star Associated with Middle Dihedral Angle	...	Star Associated with Middle Dihedral Angle
Row 6	Star Associated with Largest Dihedral Angle	Star Associated with Largest Dihedral Angle	...	Star Associated with Largest Dihedral Angle

In order to construct the non-dimensional database, the algorithm needs to first identify all the potential star triangles that fit within the frame-of-view of the star tracker. Once these triangles have been identified, their dihedral angles are computed using the equations shown in Appendix A. As shown in Table 1, the stars associated with each star triangle are sorted so that the stars at the vertices of the spherical triangle are in the same order as their corresponding dihedral angles. Each star triangle is stored in a column of the non-dimensional database.

As mentioned previously, NDSIA requires more memory than Pyramid. A comparison of the databases used by each of these algorithms quantifies this statement. Both databases were created in Python on Ubuntu 18.04 with an Intel(R) Core(TM) i5-2400 CPU at 3.10GHz with 16.0 GB of RAM. Each database

was generated from an original star catalog of 1,673 stars. The non-dimensional database took 901 seconds to generate, and contains 6 rows and 2,762,895 columns. It takes up 99.46 MB of memory. The Pyramid database took 0.175 seconds to generate, and contains 99,422 rows and 3 columns. It takes up 1.59 MB of memory, almost two orders of magnitude less memory than NDSIA. While the database generation can be done offline, so the computational time is not necessarily important, it is included here for completeness.

2.2 The Non-Dimensional Star-ID Algorithm

The identification process of NDSIA is similar to that of Pyramid [1], but with two key differences. First, NDSIA makes use of two reference stars rather than one, and second, NDSIA uses a final check at the end of the identification process that Pyramid does not. A summary of the NDSIA steps are included in the paragraphs below. Afterwards, a more detailed explanation of each step is given in its own subsection.

NDSIA begins by searching for a unique star triangle in the non-dimensional database. A unique star triangle is defined as a spherical triangle consisting of three stars whose dihedral angles match, within some given tolerance, with only one entry in the non-dimensional database. If no unique triangles exist, then no stars can be identified and the algorithm reports that it cannot identify any stars. If on the contrary, a unique triangle is found, then the algorithm continues the identification process. Let the stars in this unique star triangle be denoted as the i , j , and k star. In its next step, the algorithm searches for a reference star, r , different than i , j , or k , to verify the i , j , and k stars. If no reference star exists, the algorithm reports a failed identification. Conversely, the algorithm searches for a second reference star, r_2 . If a second reference star is found, then the i , j , k , r , and r_2 stars are identified and recorded. If no second reference star is found, then the algorithm exits and reports that no stars can be identified.

If the algorithm is able to identify the five stars i , j , k , r , and r_2 using the process mentioned above, then the remaining stars are identified using the same process performed with the first reference star. Once all stars in the frame that can be identified have been identified, the algorithm performs one final check using the interstellar angles between these identified stars, which finishes the identification process. The details of the aforementioned steps are discussed in the subsections that follow.

2.2.1 Identifying a Unique Star Triangle

A unique star triangle is a star triangle that only returns one match when searched for in the non-dimensional star database. A star triangle is identified by its dihedral angles. Thus, to find a unique star triangle, the dihedral angles must be computed using the equations in Appendix A. The dihedral angles are sorted in ascending order, to match the columns of the database, and an orthogonal range is created by adding and subtracting the quantity ϵ from the dihedral angles. Then, the NDKV orthogonal range searching algorithm [8] is used to find all possible triangles in the database that fit this range. The parameter ϵ can be used to tune the performance of NDSIA. If ϵ is smaller, the Star-ID process will be completed a lower percentage of the time, but the confidence in the Star-ID increases. If the parameter ϵ is larger, the opposite is true. In this work, ϵ is chosen to be three standard deviations of the star tracker's centroiding error. If the range search only returns one match and the L_2 norm of the difference between the spherical triangle angles in the camera frame and those in the database is less than ϵ , then that triangle is a unique star triangle. The latter of these conditions can be mathematically expressed as,

$$\sqrt{(A - A_d)^2 + (B - B_d)^2 + (C - C_d)^2} < \epsilon, \quad (1)$$

where A , B , and C are the dihedral angles computed from the camera frame and A_d , B_d , and C_d are the angles of the matching spherical triangle in the non-dimensional database. If the range search returns zero matches, more than one match, or the inequality in Eq. (1) is not satisfied, then that triangle is not a unique star triangle.

All possible combinations of three stars in the star tracker's frame-of-view are tested until a unique star triangle is identified. The method used to test all three star combinations is known as the star kernel generator. Naturally, one may be inclined to use a star kernel generator that loops through the stars in order to identify a unique star triangle. However, this is not the most efficient method. For example, if the first star in the loop is a spike (i.e. noise in the camera rather than a true star), then all triangles using that star will have to be tested before moving onto the next star. Hence, a more elegant star kernel generator is employed to ensure that all triangles are tested, but that avoids using one particular star over and over again; the pattern shifting star kernel generator from Ref. [10]. Note that the enhanced pattern shifting

star kernel generator from Ref. [10] was tested as well, but did not show any noticeable speed improvements over the pattern shifting star kernel generator for the numerical tests of NDSIA shown in this article. Future work should investigate how the myriad other star kernel generators, shifting necklace and enhanced shifting necklace to name a few, of Ref. [10] impact the performance of NDSIA.

If no unique star triangle is found, then NDSIA exits and reports it cannot identify any stars. If a reference star is found, then the algorithm moves onto the next step. Let the candidate stars of the unique star triangle found in this step be denoted as the i , j , and k stars. Let the unique star triangle itself be referred to as the $\{i, j, k\}$ triangle.

2.2.2 Identifying the First Reference Star

In order to minimize the chance of identifying stars incorrectly, two reference stars are used to verify the i , j , and k stars. Let r denote the first reference star. The first reference star is considered identified if and only if the star triangles $\{r, i, j\}$, $\{r, i, k\}$, and $\{r, j, k\}$ are unique star triangles. All stars that are not the i , j , and k stars are tested as potential reference stars until one is found. If a reference star is found, then the algorithm continues on to the next step. Otherwise, the algorithm moves back a step and continues trying to find a different set of three stars to use as the $\{i, j, k\}$ triangle.

2.2.3 Identifying the Second Reference Star

To minimize the chance of identifying stars incorrectly, a second reference star is used to verify the i , j , k , and r stars. Let r_2 denote the second reference star. The second reference star is considered identified if and only if the star triangles $\{i, j, r_2\}$, $\{i, k, r_2\}$, $\{j, k, r_2\}$, $\{i, r, r_2\}$, $\{j, r, r_2\}$, and $\{k, r, r_2\}$, are unique star triangles. All stars that are not the i , j , k , and r stars are tested as potential second reference stars until one is found. If a second reference star is found, then all five stars, i , j , k , r , and r_2 , are considered identified and are recorded. Otherwise, the algorithm moves back a step and continues trying to find a different first reference star r .

2.2.4 Identifying the Remaining Stars

After identifying the i , j , k , r , and r_2 stars, the remaining stars in the frame are identified using the same process as the first reference star. That is, for any remaining star s , that star can be identified if and only if the star triangles $\{s, i, j\}$, $\{s, i, k\}$, and $\{s, j, k\}$ are unique star triangles. If the aforementioned triangles are not unique star triangles, then that star is discarded.

2.2.5 Final Check Using Interstellar Angles

Once all the stars that can be identified have been identified, a final check is performed using the identified stars' interstellar angles. This is done by calculating the interstellar angles between every possible star pair from the subset of stars already identified. Appendix A shows how to calculate the interstellar angle between two stars. If any of the interstellar angles obtained is greater than the frame-of-view of the camera, then an error has been made in the Star-ID process. If this happens, then no stars can be accurately identified, and thus, the algorithm reports that it cannot identify any stars.

3 The Non-Dimensional Star-ID Algorithm Compared with Pyramid

In this section, NDSIA is compared with Pyramid using the following metrics:

1. Number of times that the Star-ID was completed. This metric shows whether the algorithm attempted to perform a Star-ID or not. This metric is reported as a percentage of the total number of tests.
2. Accuracy of the stars identified. This metric is calculated as the ratio of the number of times the attitude error was below three degrees to the number of times the Star-ID was completed. This ratio is reported as a percentage. This metric reflects whether the identified stars were correctly identified. Incorrect Star-IDs imply incorrect attitude estimations.
3. Average time that it takes to perform one Star-ID. This metric is reported in milliseconds.

These three metrics are used to evaluate NDSIA over a set of eight tests designed to cover different situations for the star tracker. Included below is a description of the eight tests:

- Test 1. Nominal scenario. Focal length and OA offset values are known within the maximum allowed accuracy ranges.
- Test 2. Small focal length error. The error on the focal length is 0.5% of the nominal value.
- Test 3. Large focal length error. The error on the focal length is 2.0% of the nominal value.
- Test 4. Small OA offset error. The error on the OA offset value is 0.5% of half the imager width.
- Test 5. Large OA offset error. The error on the OA offset value is 2.0% of half the imager width.
- Test 6. Small focal length and OA offset errors. The error on the focal length is 0.5% of the nominal value and the error on the OA offset value is 0.5% of half the imager width.
- Test 7. Large focal length and OA offset errors. The error on the focal length is 2.0% of the nominal value and the error on the OA offset value is 2.0% of half the imager width.
- Test 8. Small focal length and OA offset errors with larger centroiding error. The error on the focal length is 0.5% of the nominal value and the error on the OA offset value is 0.5% of half the imager width. The centroiding error used in this test has a standard deviation of 15 arcseconds. Note, this is the only test wherein a star tracker parameter differs from those shown in Table 2.

3.1 Test conditions

Each test consist of 1,000 runs, where a run consists of performing the Star-ID and calculating the spacecraft's attitude. All of the tests included in this section were performed in C++ on a computer running Ubuntu 18.04 with an Intel(R) Core(TM) i5-2400 CPU at 3.10GHz with 16.0 GB of RAM. All run times were calculated using the system_clock function in the C++ boost chrono library. The parameters of the virtual star tracker used in these tests are shown in Table 2, where $U[0, 5]$ represents the uniform distribution of integers in the range $[0, 5]$ and σ denotes the standard deviation of a normal distribution.

Table 2: Star tracker parameters

Virtual Star Tracker Parameter	Value
1 σ centroid error	10 arcseconds
Star magnitude threshold	5.0
Number of spikes (false stars)	$U[0, 5]$
Number of rows pixels	1,024
Number of columns pixels	1,024
Pixel pitch	0.018 mm
Focal length	50.47 mm

The centroiding error was applied to the star measurements in the camera frame using the methodology shown in Eq. (2).

$$\begin{aligned}
 \theta &\sim \mathcal{N}(0, \sigma^2) \\
 \mathbf{e} &= \mathbf{v} \times \hat{\mathbf{b}}_t \\
 \hat{\mathbf{e}} &= \mathbf{e} / \|\mathbf{e}\| \\
 C_p &= C_p(\hat{\mathbf{e}}, \theta) \\
 \hat{\mathbf{b}}_e &= C_p \hat{\mathbf{b}}_t
 \end{aligned} \tag{2}$$

where $\mathcal{N}(\mu, \sigma^2)$ is the normal distribution with mean μ and variance σ^2 , σ is the centroid error of the camera, 10 arcseconds, $\hat{\mathbf{b}}_t \in \mathcal{R}^3$ is unit vector that points to the true direction of the star in the camera reference frame, $\hat{\mathbf{b}}_e \in \mathcal{R}^3$ is the observed unit vector, affected by centroid error, $\mathbf{v} \in \mathcal{R}^3$ is a random vector, and the

function $C_p(\hat{\mathbf{e}}, \theta)$ is the attitude matrix where $\hat{\mathbf{e}}$ is the principle axis and θ the principle angle. The function used to calculate C_p given $\hat{\mathbf{e}}$ and θ is,

$$C_p(\hat{\mathbf{e}}, \theta) = \mathcal{I}_{3 \times 3} \cos \theta + (1 - \cos \theta) \hat{\mathbf{e}} \hat{\mathbf{e}}^T - [\hat{\mathbf{e}} \times] \sin \theta$$

where $\mathcal{I}_{3 \times 3}$ is the 3×3 identity matrix and $[\hat{\mathbf{e}} \times]$ is the skew-symmetric matrix formed using the components of $\hat{\mathbf{e}}$.

The focal length and OA offset perturbations are applied to the star measurements in the camera frame using the methodology shown in Eq. (3),

$$\begin{aligned} \begin{Bmatrix} x_c \\ y_c \end{Bmatrix} &= \begin{bmatrix} -f - \delta f & 0 & 0 \\ 0 & -f - \delta f & 0 \end{bmatrix} \frac{\hat{\mathbf{b}}_e}{\hat{\mathbf{b}}_e(3)} \\ \mathbf{b}_p &= \begin{Bmatrix} \pm x_c - x_{oa} + \delta x \\ \pm y_c - y_{oa} + \delta y \\ f + \delta f \end{Bmatrix} \\ \hat{\mathbf{b}}_p &= \frac{\mathbf{b}_p}{|\mathbf{b}_p|}, \end{aligned} \quad (3)$$

where $\hat{\mathbf{b}}_e(3)$ is the third component of the vector $\hat{\mathbf{b}}_e$, δf is the focal length perturbation, δx and δy are the OA offset perturbations, and $\hat{\mathbf{b}}_p$ is the unit vector pointing to the star whose centroid coordinates are $[x_c, y_c]$ on the imager. The “ \pm ” sign appearing in Eq. (3) depends on the imager x and y axes directions. Note that Eq. (3) assumes that the star tracker is modelled as an ideal pin-hole camera.

3.2 Results

Table 3 gives a summary of the performances and results of Pyramid and NDSIA on these eight tests. For each algorithm, three columns are included that contain the three metrics described earlier. The first column, $n_{id}(\%)$, gives the percentage of runs where the star-ID was completed, and the second column, $n_{<3^\circ}$, shows the percentage of completed star-ID runs with an attitude error less than 3° . The third column gives the average run time of each algorithm in milliseconds.

Table 3: Comparison between the Pyramid algorithm and NDSIA

Test number	Pyramid			Non-Dimensional		
	$n_{id} (\%)$	$n_{<3^\circ} (\%)$	t_{avg} (ms)	$n_{id} (\%)$	$n_{<3^\circ} (\%)$	t_{avg} (ms)
Test 1	100.000	100.000	0.139	84.200	100.000	2.812
Test 2	41.800	96.651	10.833	79.400	100.000	3.799
Test 3	9.200	50.000	27.778	21.500	100.000	24.261
Test 4	100.000	100.000	0.141	81.800	100.000	3.403
Test 5	100.000	100.000	0.140	53.500	100.000	12.606
Test 6	41.700	96.163	10.887	77.200	100.000	4.319
Test 7	10.200	42.157	27.641	14.700	100.000	29.381
Test 8	75.500	96.026	6.918	75.900	100.000	7.057

Test 1 shows that when the star tracker is working nominally Pyramid and NDSIA are each able to identify the stars correctly. However, Pyramid is able to identify stars more often than NDSIA and Pyramid is more than an order of magnitude faster than NDSIA. This is expected, as NDSIA is meant to be used only when the Pyramid algorithm begins to fail.

Test 2 and Test 3 are the first two examples of such situations. These tests were performed with focal length perturbations. Compared to the nominal case, the Pyramid algorithm performance degrades significantly. The most alarming change in the performance of the Pyramid algorithm is the percentage of tests with an attitude error less than three degrees. In Test 2 and Test 3, the attitude based on Pyramid’s Star-ID can no longer be trusted. In contrast, the percentage of tests with an attitude error of less than three degrees given by the NDSIA remains unchanged from the nominal case. However, the number of Star-IDs that can

be completed is reduced significantly when compared with the nominal case. In addition, the time required to complete a Star-ID increases due to the focal length perturbations.

In Test 4 and Test 5, the performance of the Pyramid algorithm remains almost unchanged when compared with Test 1 (star tracker working nominally). The reason for that is that small OA offset perturbations have little effect on the interstellar angles between stars for most locations on the imager. Therefore, the Pyramid algorithm is still able to perform the Star-ID in every case. Conversely, the small OA offset perturbations have a larger effect on the dihedral angles between the stars. Thus, the number of times that the Star-ID can be completed by the NDSIA is reduced as the OA offset increases. However, the percentage of tests with an attitude error less than three degrees remains unchanged from the nominal case. Therefore, while the NDSIA may not be able to perform the Star-ID process as often as Pyramid when there is an OA offset, the attitude given by the NDSIA can still be trusted.

Test 6 and Test 7 show the performance of the two algorithms when subject to both focal length perturbations and OA offset perturbations. In these two tests, there is again a significant degradation in the performance of the Pyramid algorithm. Also, while the number of Star-IDs that the NDSIA can complete is reduced when compared with Test 1 (nominal case), the percentage of tests with an attitude error of less than three degrees remains unchanged.

Test 8 shows that NDSIA is robust to changes in the centroiding accuracy of the camera, because the performance of NDSIA in Test 8 is similar to the performance of NDSIA in Test 6 (Test 6 is the same as Test 8 but with a lower centroiding error). Comparing Pyramid and NDSIA on Test 8 reveals that NDSIA does better in terms of percentage of star-IDs completed and percentage of completed star-IDs with an attitude error less than three degrees. The Pyramid algorithm is slightly faster than NDSIA in Test 8. Comparing the Pyramid results for Test 8 with the Pyramid results for Test 6 shows that Pyramid is able to perform more star IDs in Test 8 than Test 6. The larger centroiding error absorbs some of the error due to the focal length and OA offset perturbations. In other words, in many cases, the position error of stars in the camera frame due to focal length and OA offset perturbations is less than the typical centroiding error in Test 8. Thus, with the increased centroiding error and therefore an increased range when performing the associated range searches, Pyramid is able to identify the stars in more cases.

Based on the results of Test 8, one is naturally led to wonder if the performance of Pyramid can be improved by increasing the range it uses when performing range searches in its database. Note, that in Test 8 both the actual camera centroiding error and the range used in Pyramid were modified. In contrast, here, only the range Pyramid uses will be modified, the actual camera centroiding error will be held constant, using the value given in Table 2. Table 4 shows how the performance of Pyramid is impacted by changing the size of the range search. The left most column in 4 gives the standard deviation, σ , that Pyramid assumes the star tracker camera has; hence, the range that Pyramid uses when searching the database of interstellar angles is $\pm 3\sigma$. The focal length and OA offset perturbations used to create Table 4 are the same as those used in Test 6. Hence, the first row of Table 4 is identical to that of Test 6. Each row in Table 4 was created using 1,000 runs of the Pyramid algorithm, the same as in the previous 8 tests. Table 4 shows that as the

Table 4: Pyramid performance as a function of range search size

σ used for Pyramid range search	n_{id} (%)	$n_{<3^\circ}$ (%)	t_{avg} (ms)
10	41.7	96.163	10.887
15	74.6	96.515	7.155
20	93.3	95.498	3.629
25	98.2	94.603	2.648
30	99.3	95.972	2.931
35	99.8	94.890	4.045
40	99.9	94.494	7.264

range that Pyramid uses increases, so does the percentage of tests for which it can identify the stars. The percentage of successful star IDs for which the attitude error is less than three degrees decreases slightly as the range that Pyramid uses increases. As a result, the total number of tests for which Pyramid identifies stars such that the attitude estimation is less than three degrees is similar for the last 4 rows in Table 4. However, note that at no point is the accuracy of the Pyramid algorithm as good as that of NDSIA for Test 6. Moreover, for each test in Table 4 there are still a notable number of cases for which Pyramid identifies

stars incorrectly. Hence, even by varying the range that Pyramid uses to search in the database, the Pyramid algorithm does not outperform NDSIA.

Histograms of attitude error are provided for each test to quantify how much the perturbations affect the attitude estimation. Figures 1 and 2 show the histograms of attitude error for Pyramid and NDSIA for Test 1. These figures show that the two algorithms have similar attitude error distributions, but with Pyramid having more Star-IDs completed than NDSIA.

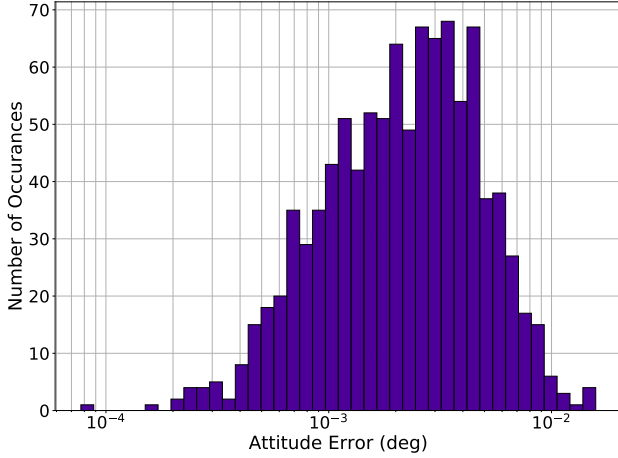


Figure 1: Test 1: Pyramid

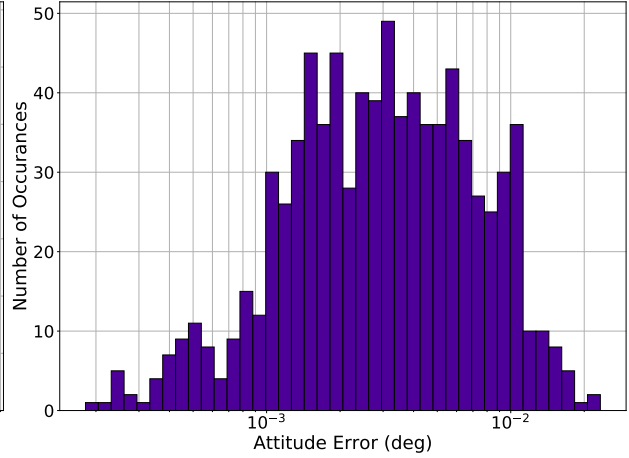


Figure 2: Test 1: NDSIA

Figures 3 through 6 show histograms of the attitude error for Pyramid and NDSIA for Test 2 and Test 3. These histograms clearly show that NDSIA is more accurate on average than the Pyramid algorithm. Moreover, comparing Test 2 and Test 3 to Test 1 reveals that the attitude error of NDSIA increases slightly as the focal length perturbation increases; however, there are no tests with an attitude error above three degrees.

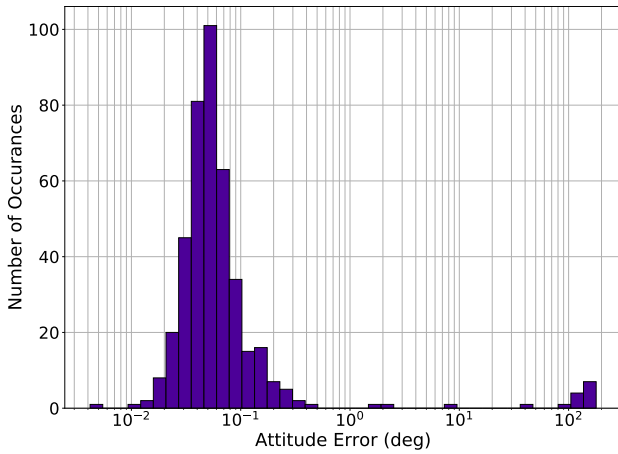


Figure 3: Test 2: Pyramid

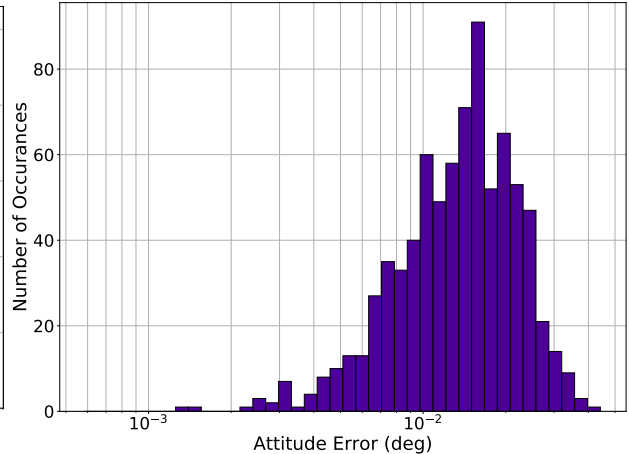


Figure 4: Test 2: NDSIA

Figures 7 through 10 show the attitude error histograms for Pyramid and NDSIA for Test 4 and Test 5. These figures show that the attitude error distributions for the two algorithms are similar for both tests; however, in each case, NDSIA completed less Star-IDs than the Pyramid algorithm. When compared to Test 1, the attitude error of both algorithms increases with the increase in the OA offset perturbation.

Figures 11 through 14 show the attitude error histograms for Pyramid and NDSIA for Test 6 and Test 7. These figures show that on average NDSIA is more accurate than Pyramid. In these tests, NDSIA is able to complete the Star-ID process in more cases than Pyramid.

Figures 15 through 16 show the attitude error histograms for Pyramid and NDSIA for Test 8. These figures show that on average NDSIA is more accurate than Pyramid. In Test 8, NDSIA was able to complete

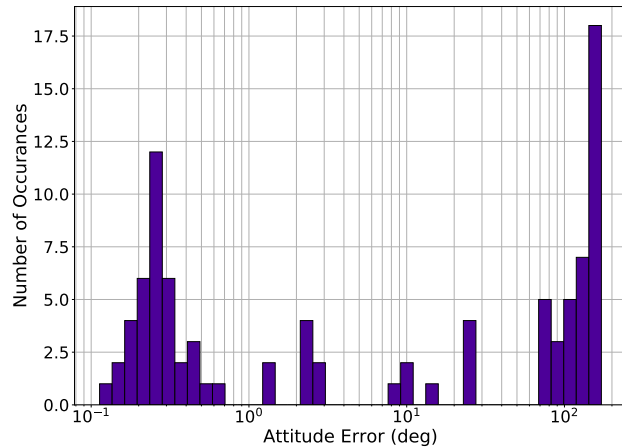


Figure 5: Test 3: Pyramid

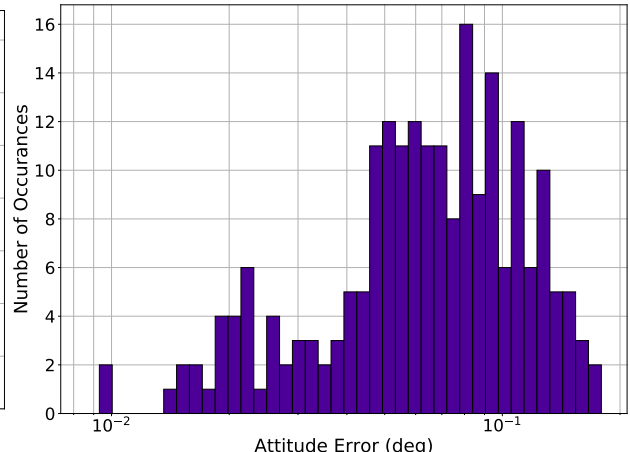


Figure 6: Test 3: NDSIA

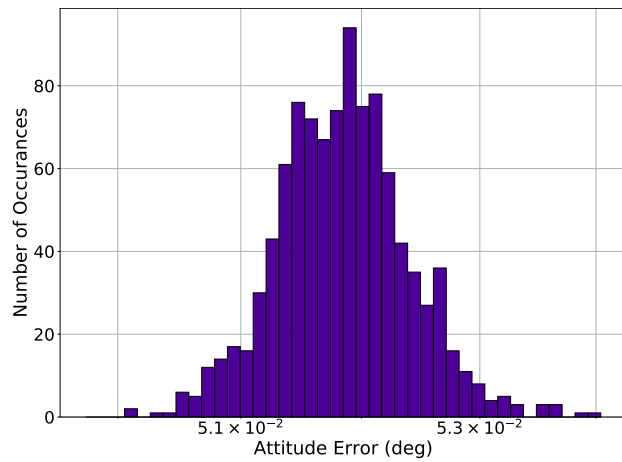


Figure 7: Test 4: Pyramid

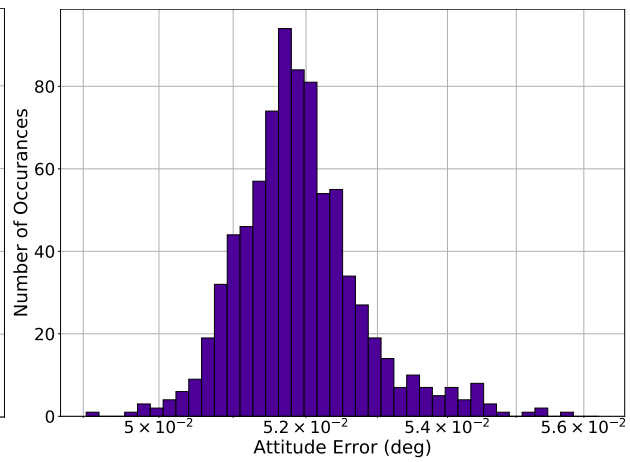


Figure 8: Test 4: NDSIA

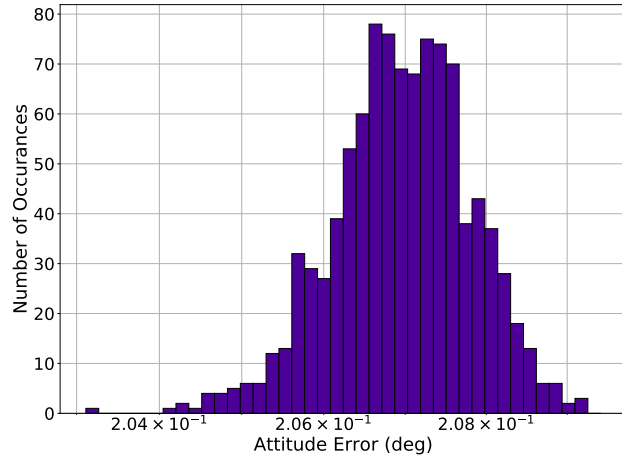


Figure 9: Test 5: Pyramid

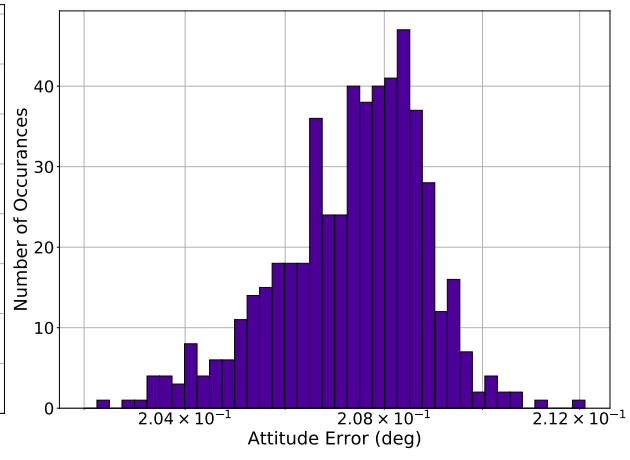


Figure 10: Test 5: NDSIA

the Star-ID process more times than Pyramid. Comparing the results of this test with Test 6 reveals that the performance of NDSIA is similar between the two tests, while the Pyramid performance improves noticeably in Test 8.

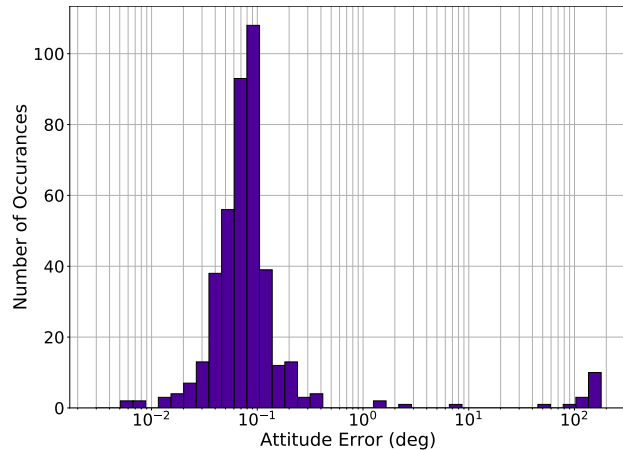


Figure 11: Test 6: Pyramid

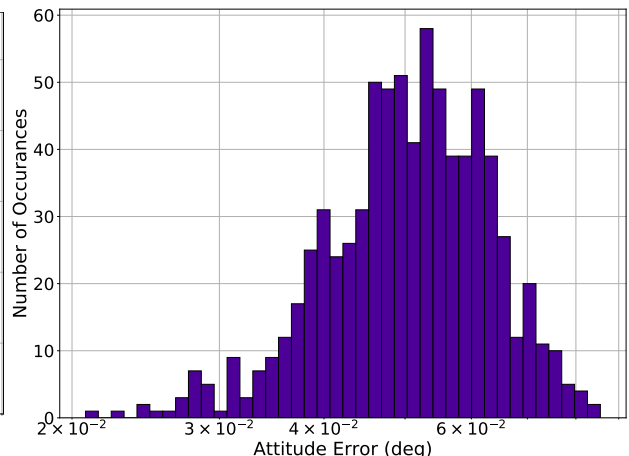


Figure 12: Test 6: NDSIA

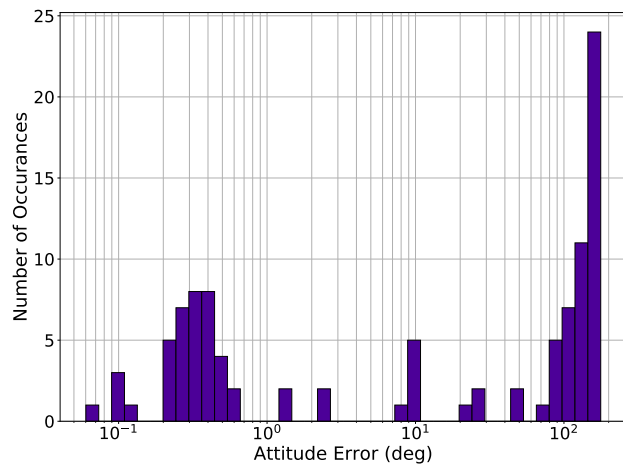


Figure 13: Test 7: Pyramid

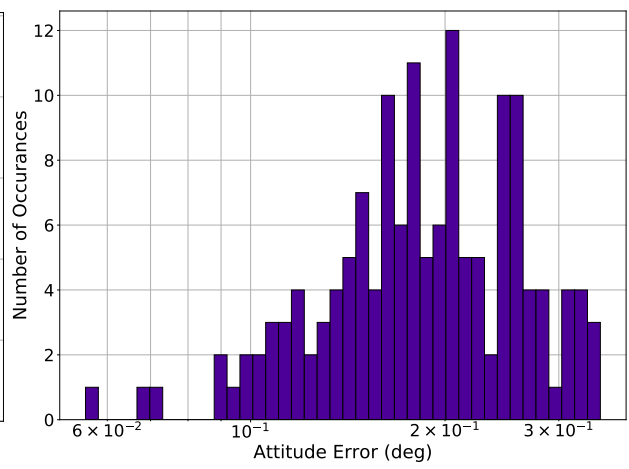


Figure 14: Test 7: NDSIA

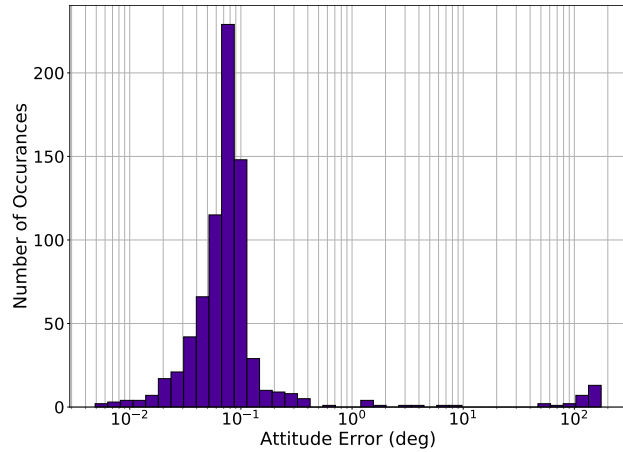


Figure 15: Test 8: Pyramid

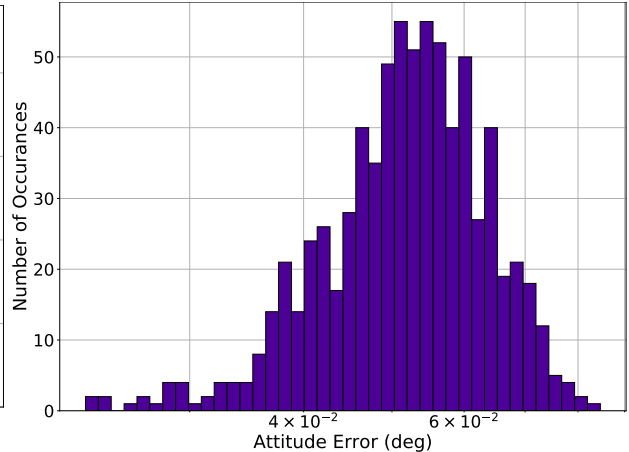


Figure 16: Test 8: NDSIA

4 Conclusions

This work introduces the Non-Dimensional Star-Identification Algorithm (NDSIA), a real-time star identification algorithm for star trackers on-board spacecraft. NDSIA is devised to complement other nominal

lost-in-space algorithms (NLISA), for instance Pyramid. When NLISA fails due to perturbations of the focal length and/or the OA offset in the star tracker, NDSIA is still able to identify stars. Moreover, not only can NDSIA be used to identify stars when NLISA fails, it can be used to re-calibrate the star tracker.

The idea behind NDSIA is to identify stars via a database containing information about spherical star triangles that can be generated from a set of stars in a star catalogue. In particular, each element from this database contains both the stars that generated the star triangle, and values of the dihedral angles that these stars form in a unit 3D sphere. Each time that an identification is required, three candidate stars from the frame are selected and checked against the database. If a unique match is found, then two additional stars, called reference stars, from the frame are selected and used to generate all nine possible star triangles between each reference star and the stars in the original triangle. If these nine star triangles also produce unique matches in the database, then the algorithm identifies this subset of 5 stars. The original three stars are used to continue with the identification of the remaining candidate stars from the image. Each remaining star is identified using a process similar to the first reference star. Finally, once the process is finished, the interstellar angles between each pair of identified stars is used as a final check to ensure the star identification was performed correctly.

It is important to note that in order to perform the identification of a star triangle in the algorithm database, a three-dimensional search is required, where each dimension of the search corresponds to each one of the dihedral angles included in the database. Using a three-dimensional database significantly reduces the number of star triangle combinations for a given dihedral angle tolerance at the cost of making the searching process more difficult. Nevertheless, the increased search difficulty is solved in NDSIA by using the n -dimensional k -vector (NDKV) algorithm.

Through a series of eight tests in this article, NDSIA was demonstrated to be robust to changes in both the focal length and OA offset of a star tracker, providing an accurate spacecraft attitude even when these camera parameters were perturbed. In contrast, algorithms like Pyramid showed an alarming increase in incorrect star identifications when subject to focal length perturbations. Under perturbations just in the OA offset, the tests performed in this work showed little effect on Pyramid.

One important property of NDSIA is that the algorithm can be used to compute the new values of the focal length and/or OA offset of the star tracker camera. Using this information, it is possible to update the star database on-board the spacecraft to take into account these perturbations. That way, the nominal star identification algorithm, which usually has a better speed performance and lower computational cost, can be used again as it is more efficient.

Finally, the results presented in this work show that using a combination of Pyramid and NDSIA algorithms provides a fast and robust methodology for dealing with the real-time star identification problem even under the effect of perturbations in the focal length and/or the OA offset of star trackers. Together, the strengths of one algorithm complement the weaknesses of the other, increasing the reliability of the system as a whole.

Acknowledgments

This work was supported by a NASA Space Technology Research Fellowship, Leake [NSTRF 2019] Grant #: 80NSSC19K1152.

A Interstellar and Dihedral Angles of Spherical Star Triangles

Figure 17 shows a spherical triangle. The angles a , b , and c are interstellar angles, the angles between two stars. Angles A , B , and C are the dihedral angles of the spherical triangle formed by these three star pairs.

The interstellar angles can be calculated using Eq. (4).

$$\begin{cases} a = \cos^{-1} (\hat{\mathbf{b}}_B^T \hat{\mathbf{b}}_C) \\ b = \cos^{-1} (\hat{\mathbf{b}}_A^T \hat{\mathbf{b}}_C) \\ c = \cos^{-1} (\hat{\mathbf{b}}_A^T \hat{\mathbf{b}}_B) \end{cases} \quad (4)$$

where $\hat{\mathbf{b}}_A$ is the unit-vector from the origin to the star located at A , $\hat{\mathbf{b}}_B$ is the unit-vector from the origin to the star located at B , and $\hat{\mathbf{b}}_C$ is the unit-vector from the origin to the star located at C .

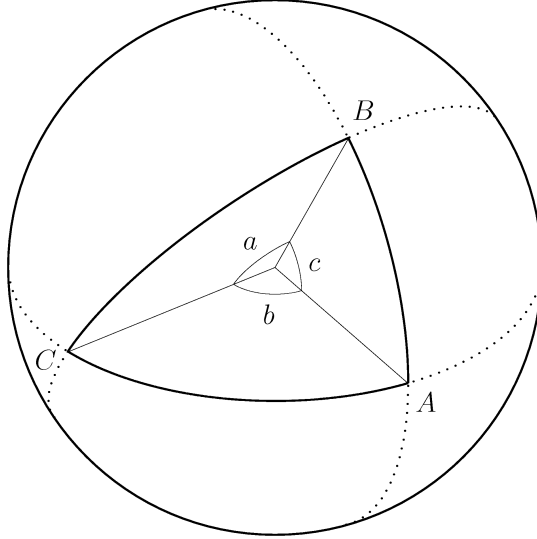


Figure 17: Spherical Triangle

The way the dihedral angles are calculated depends on which of the interstellar angles is the smallest. If a is the smallest angle, then the first line of Eq. (5) is used. If b is the smallest angle, then the second line of Eq. (5) is used. If c is the smallest angle, then the third line of Eq. (5) is used.

$$\begin{cases} A = \cos^{-1} \left(\frac{\cos a - \cos b \cos c}{\sin b \sin c} \right) \\ B = \cos^{-1} \left(\frac{\cos b - \cos a \cos c}{\sin a \sin c} \right) \\ C = \cos^{-1} \left(\frac{\cos c - \cos a \cos b}{\sin a \sin b} \right) \end{cases} \quad (5)$$

Once one of the dihedral angles is calculated using Eq. (5), the remaining two dihedral angles are calculated using Eq. (6).

$$\frac{\sin A}{\sin a} = \frac{\sin B}{\sin b} = \frac{\sin C}{\sin c} \quad (6)$$

The attentive reader will notice that this method of calculating the dihedral angles involves an ambiguity, as the inverse sine function will only return positive answers between 0 and $\pi/2$, when a dihedral angle may be larger than $\pi/2$. This ambiguity can be avoided by using a tangent rule to calculate the remaining two dihedral angles. To test the effect of this ambiguity, all of the tests shown in this article were completed using the sine rule and the tangent rule, and there were no differences in the percentage of star-IDs completed nor in the percentage of star-IDs with an attitude error less than three degrees when using the tangent rule versus the sine rule. Moreover, when using the tangent rule, the computational time always increased compared to when using the sine rule; in one case, the average computational time was four times larger when using the tangent rule than when using the sine rule. Thus, for all data reported in this article, the sine rule was always used to calculate the larger two dihedral angles.

References

- [1] Daniele Mortari, Christian Bruccoleri, and John Lee Junkins. The *Pyramid* Star Identification Technique. *ION Navigation*, 51(3):171–183, 2004.
- [2] Daniele Mortari. A Fast On-Board Autonomous Attitude Determination System Based on a New Star-ID Technique for a Wide FOV Star Tracker. In *AAS/AIAA Space Flight Mechanics Meeting*, Austin, TX, February 1996.

- [3] Daniele Mortari and Beny Neta. k -vector Range Searching Techniques. In *Advances in the Astronautical Sciences*, volume 105, Pt. I, pages 449–464, 2000.
- [4] Malak Samaan, Daniele Mortari, and John Lee Junkins. Non-Dimensional Star Identification for Uncalibrated Star Cameras. *The Journal of the Astronautical Sciences*, 54(1):95–111, 2006.
- [5] Benjamin B. Spratling and Daniele Mortari. The k -vector ND and its Application to Building a Non-Dimensional Star-ID Catalog. *The Journal of the Astronautical Sciences*, 58:261–274, 2011.
- [6] G. Lamy Au Rousseau, J. Bostel, and B. Mazari. Star recognition algorithm for APS star tracker: oriented triangles. *IEEE Aerospace and Electronic Systems Magazine*, 20(2):27–31, February 2005. doi: 10.1109/maes.2005.1397146.
- [7] Mohamad Javad Ajdadi, Mahdi Ghafarzadeh, Mojtaba Taheri, Ehsan Mosadeq, and Mahdi Khakian Ghomi. Star Identification Algorithm for Uncalibrated, Wide FOV Cameras. *The Astronomical Journal*, 149(6):182, May 2015. doi: 10.1088/0004-6256/149/6/182.
- [8] David Arnas, Carl Leake, and Daniele Mortari. The n -dimensional k -vector and its application to orthogonal range searching. *Applied Mathematics and Computation*, 372:125010, 2020. ISSN 0096-3003. doi: 10.1016/j.amc.2019.125010.
- [9] F. Somayehee, A. A. Nikkhah, J. Roshanian, and S. Salahshoor. Blind star identification algorithm. *IEEE Transactions on Aerospace and Electronic Systems*, pages 1–1, May 2019. ISSN 0018-9251. doi: 10.1109/TAES.2019.2917572.
- [10] David Arnas, M'arcio A.A. Fialho, and Daniele Mortari. Fast and robust kernel generators for star trackers. *Acta Astronautica*, 134:291–302, 2017. ISSN 0094-5765. doi: 10.1016/j.actaastro.2017.02.016.